High harmonic lasing using attosecond electron pulse combs in photon-induced near-field electron microscopy

Yiming Pan[1], Ido Kaminer[2], Michael Krueger[1]

Contact:
yiming.pan@campus.technion.ac.il

1. Physics Department and Solid State Institute, Technion, 32000 Haifa, Israel
2. Department of Electrical and Computer Engineering, Technion, 32000 Haifa, Israel

ABSTRACT

Attosecond laser pulses in the extreme ultraviolet/soft X-ray (XUV/SXR) spectral regions are presently available for attosecond pump-probe spectroscopy and extreme ultraviolet lithography for chip manufacturing, ultrafast atomic-scale microscopy, and nonlinear X-ray optics. There are two main approaches to produce attosecond light pulses: high-harmonic generation (HHG) in gas-phase or solid-state matter based on the three-step model [1-3], and X-ray free-electron lasers (XFELs) based on self-amplified spontaneous emission (SASE) and laser seeding processes of relativistic free electrons traveling through an undulator [4,5].

Here, we propose a novel route of producing attosecond laser pulses, based on the generation of attosecond electron pulse trains in photon-induced near-field electron microscopy (PINEM) [6-8], combined with the SASE principle for light amplification. Our scheme relies on high-density nanotip arrays emitting dense electron bunches [9] that are subsequently modulated with a PINEM-type interaction, enabling high-gain for amplification of XUV/SXR high harmonic radiation.

SETUP of PINEM-HHG

In analogy with the three-step model of HHG (ionization, acceleration, and recombination of an initially bound electron), we call our PINEM-HHG laser scheme the "three-tip" model (see Fig. 1a), which can create both attosecond electron pulses and attosecond light pulses in a phase-coherent manner: the first tip emits electron pulses triggered by femtosecond laser pulses, with up to 10^2 electrons per laser pulse per tip [10]; the second tip modulates the electrons through a PINEM interaction with IR light (~800 nm) [7] and creates periodically bunched attosecond electron pulses [11]; the last tip serves as a radiation antenna for generating attosecond XUV/SXR pulses when interacting with the electron pulse train. Our scheme thus combines a tip emitter, a tip modulator, and a tip radiator.

In order to enhance the attosecond radiation power further, we replace the three tips with high-density nanotip arrays. The first tip is replaced by a 2D array (pitch of 100 nm) for generating a high electron charge density, thereby increasing it from 10^2 to 10^7 per laser pulse [9]. We also increase the PINEM interaction time (increasing the interaction length to 100 nm, with acceleration gradient field 1GV/m) by introducing an array modulator with ten nanotips (pitch of 100 nm). As a result, we can achieve the widely spread PINEM spectrum of the order of a few hundred electron volts, which as a crucial parameter limits the cutoff frequency of the radiation. Indeed, we find a linear scaling law of the cutoff frequency because it linearly depends on the laser-induced energy spread. At last, we realize SASE of XUV/SXR lasing radiation with an array radiator with 100 nanotips with a pitch of 800 nm (to match the period of electron pulse trains), respectively.

RESULTS

In order to assess the efficiency of PINEM-HHG, we devise a fully quantum theory approach based on quantum electrodynamics in the strong-field regime.

Typical features of PINEM-HHG are shown in Fig. 1b-1d. Fig. 1b shows the HHG spectrum from an attosecond bunched free electron with PINEM spectrum with a spread of 160 eV. The HHG spectrum has a plateau shape and a cutoff at harmonic order $n_{cutoff} = 150$, corresponding to the PINEM spread. Fig. 1c shows the linear dependence of the cutoff frequency on the laser coupling strength $2|g|$ and hence on the laser field strength, similar to the linear power law of solid-state HHG [3]. A Fourier transform to the time domain reveals a radiative attosecond pulse train (see Fig. 1d). We find that the pulse duration in the trains is 20 as, which is on the order of the atomic unit of time (inset of Fig. 1d) and can hardly be achieved from FEL of relativistic beams [12].

In total, the best-case theoretical estimation of the superradiant XUV/SXR photon emission is $N_{ph} = \left(N_e N_{tip_3}\right)^2 \Delta\nu_{sp} \sim 10^{11}$ photon/pulse, with $N_e = 10^7, N_{tip_3} = 100$ [9] and the emitted photon number per single electron $\Delta\nu_{q,sp} \sim 10^{-7}$. The N_e^2-dependence stems from the superradiance where many electrons emit coherently, and the $N_{tip_3}^2$-dependence from the SASE process when the photons are emitted spontaneously from the attosecond electron pulses and radiation emission builds up exponentially, until saturation. It is worthy to compare with the practical assessment of the first lasing in LCLS ($\sim 10^{13}$ photon/pulse), in which the beam has bunched electrons of the order of 10^9 [5].

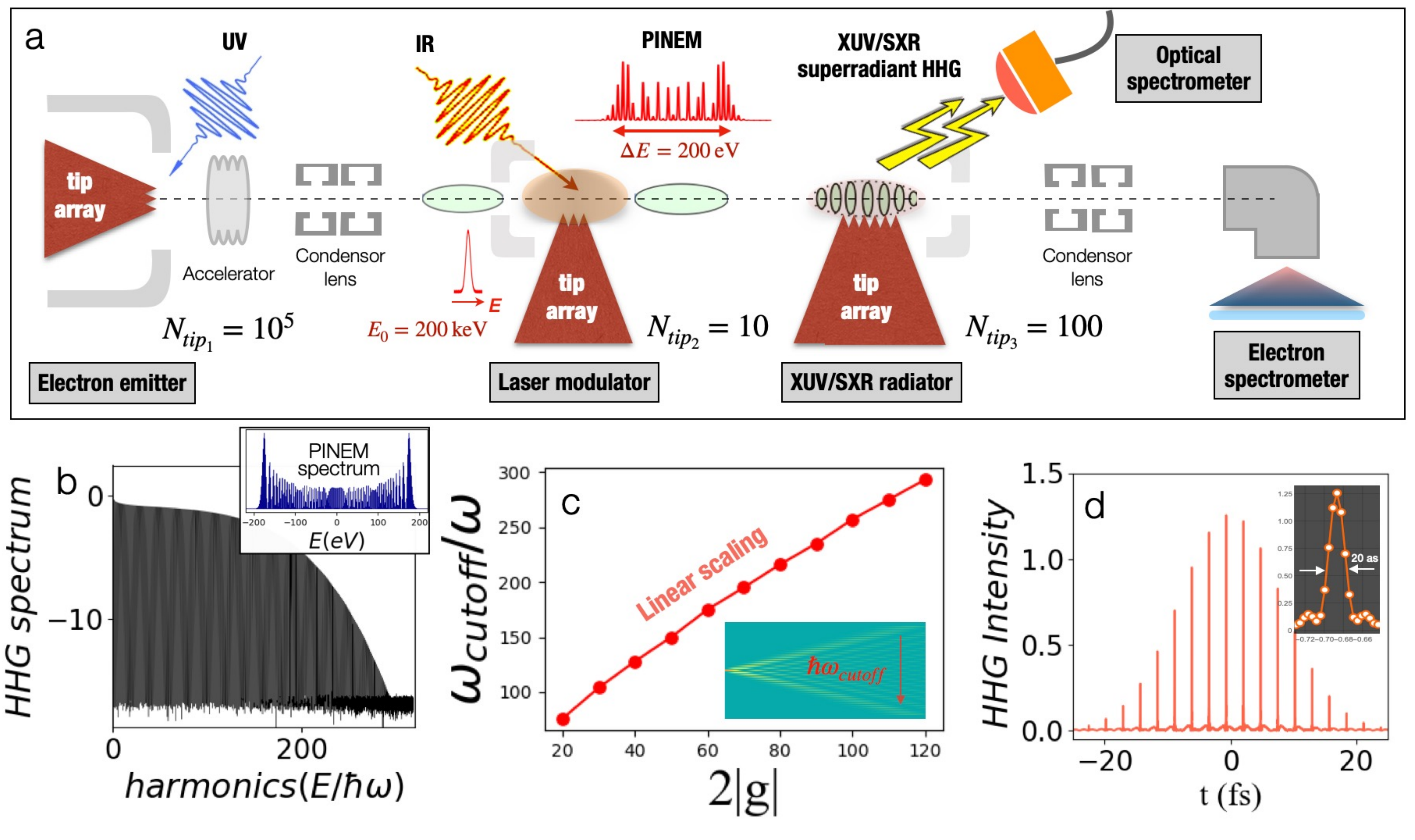

Fig. 1: **The setup and concept of PINEM-HHG lasing.**

(a) The "three-tip" model of PINEM-HHG scheme.

(b) The HHG spectrum from PINEM-induced attosecond bunched free electrons. The inset is the corresponding PINEM spectrum.

(c) The linear scaling law of the HHG cutoff frequency.

(d) The generation of attosecond PINEM-HHG laser pulse trains in the XUV/SXR region.

OUTLOOK

We will realize our ambitious PINEM-HHG lasing scheme in two steps:

- The first step is to generate both a phase-coherent attosecond electron pulse train and an attosecond XUV/SXR light pulse and correlate them with each other. Since both the electron and light pulses stem from a simultaneous interaction process at the nanotip array radiator, the electrons and photons are coherently phase-correlated and spectrally entangled at the quantum-mechanical level. As a result, the free electron and laser pulses can be used as a promising tool of attosecond pump-probe experiments further to explore ultrafast and subatomic electron dynamics in condensed matters.
- The second step is to produce the attosecond laser as the next generation of state-of-the-art sources, which can trigger further applications of nonlinear X-ray optics and strong-field plasma physics.

REFERENCES

[1]. Corkum, Paul B. (1993). PlPhys. Rev. Lett. 71.13, 1994. [2]. Paul, P. M., et al. (2001). Science, 292(5522), 1689-1692. [3]. Ghimire, S., et al. (2011). Nature Physics, 7(2), 138-141. [4]. Madey, J. (1971). J. Appl. Phys. 42, 1906–1913. [5]. Emma, P., et al. (2010). Nature Photonics, 4(9), 641-647. [6]. Barwick, B., et al. (2009). Nature, 462(7275), 902-906. [7]. Feist, A., & Ropers, C. (2015). Nature, 521(7551), 200-203. [8]. Dahan, R., & Kaminer, I. (2020). Nature Physics, 16(11), 1123-1131. [9]. Mustonen, A., & Tsujino, S. (2011). Appl. Phys. Lett. 99(10), 103504. [10]. Bormann, R., & Ropers, C. (2010). Phys. Rev. Lett. 105(14), 147601. [11]. Priebe, K. E., & Ropers, C. (2017). Nature Photonics, 11(12), 793-797. [12]. Huang, S., & Zhu, D. (2017). Phys. Rev. Lett. 119(15), 154801.